2018 European Control Conference (ECC)
June 12-15, 2018. Limassol, Cyprus

Prioritization-based switched feedback control for linear SISO systems with time-varying state and input constraints

Steffen Joos⋆, Matthias Bitzer⋆, Roland Karrelmeyer⋆ and Knut Graichen†

Abstract— **The problem of stabilization by means of state feedback is discussed for linear single input single output systems while satisfying time-varying polytopic constraints on both the states and the control input. The core of the switched control concept derived in this work is a standard state feedback controller, stabilizing the system in the unconstrained case, whereas its control signal is optimally limited in order to achieve feasibility of the states and the input in the constrained case. For the derivation of the limiting function, feasible dynamic limits are designed which correspond to one additional control law per constraint. A switching logic for these limits is then constructed with the solution of an optimization problem. Thereby, an explicit order of constraints prioritization is taken into account in order to obtain a unique switching logic. Throughout the derivation, the property of differential flatness is exploited, which allows the reduction of the respective system to the control of a (constrained) integrator chain. The performance of the control approach as pure feedback as well as in a constrained two-degree-of-freedom setup is finally discussed by means of simulation studies. Furthermore, a comparison of the achieved results with a model predictive control approach is carried out.**

I. Introduction

Constraints of both states and inputs are present in all technical control problems, hence incorporating constraints during the control design is an ongoing subject of research. In the literature, there exist various types of approaches for the incorporation of constraints in the feedback control scheme. One approach is to vary the feedback controller online using e.g. (soft) variable structure control [1] or model predictive control (MPC) methods [2], [3]. These methods result basically in a time-variant feedback gain. Another possibility is to make use of anti wind-up concepts [4], [5]. All these concepts have certain drawbacks like for instance the computational burden for MPC or the incompatibility of the other feedback concepts concerning their integration within a constrained two-degree-of-freedom (2DOF) structure, i.e. in combination with a constrained (online) trajectory planning [6] and a respective feedforward controller.

The contribution of this paper is the derivation of a switched feedback controller (SFC) for linear SISO systems with minimum phase behavior [7] consisting of a state feedback which is dynamically limited in order to account for time-variant state and input constraints. Fig. 1 sketches the basic control structure which is successively detailed in the course of this work. The main target of the presented design is to combine the advantages of differential flatness [8], optimization based concepts [9] in terms of optimal control behavior, and switched systems [10] as a contribution for the above introduced control problem for constrained systems. A fixed order of constraints prioritization is further incorporated in the controller design and allows a unique handling of temporarily infeasible situations, where e.g. constraints are contradictory.

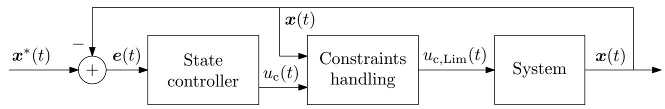

Fig. 1. Structure of the considered setup consisting of a linear system controlled with a state feedback and the optimal limitation of the control signal u_c derived in this work in order to consider constraints.

The present paper is organized as follows: In Sec. II, the problem is stated and the system theoretic property of differential flatness is briefly summarized. Further, Sec. III both revises the design of state feedback controllers for the unconstrained case as well as introduces and discusses feasible system dynamics for the constrained case with respect to its utilization for the derivation of the SFC in Sec. IV. Thereby, a novel (switched) control architecture is derived by means of an optimization problem and a prioritization of constraints. In Sec. V, the performance and the robustness of the derived control approach as well as its integration in a constrained 2DOF-structure with online trajectory planning [6] is demonstrated by means of simulation studies. Sec. VI concludes the paper and points out future work aspects.

II. Problem statement

The present section first introduces the plant along with the time-variant state and input constraints in Sec. II-A, followed by a brief recall of differential flatness in Sec. II-B with respect to its utilization for the parametrization of the constrained system.

A. Definition of the constrained system

In the sequel, controllable linear SISO systems

$$\dot{\boldsymbol{x}}(t) = \boldsymbol{A} \cdot \boldsymbol{x}(t) + \boldsymbol{b} \cdot u(t), \ t > 0, \ \boldsymbol{x}(0) = \boldsymbol{x}_0 \tag{1a}$$

$$y(t) = \boldsymbol{c}^{\mathrm{T}} \cdot \boldsymbol{x}(t), \qquad t \geq 0 \tag{1b}$$

with the state $\boldsymbol{x}(t) \in \mathbb{R}^n$, the input $u(t) \in \mathbb{R}^1$ and the output $y(t) \in \mathbb{R}^1$ are considered. Furthermore, it is assumed that the plant (1) exhibits minimum phase behavior [7], [11]. As state constraints[1], time-variant polytopic constraints of the form

$$P_x = \{\boldsymbol{x} \in \mathbb{R}^n : \quad \boldsymbol{F}_x \cdot \boldsymbol{x}(t) - \boldsymbol{g}_x(t) \leq \boldsymbol{0}\} \tag{2a}$$

[1]Note that time-varying output constraints can be expressed as state constraints according to $y_{\min}(t) \leq y(t) = \boldsymbol{c}^{\mathrm{T}} \cdot \boldsymbol{x}(t) \leq y_{\max}(t)$.

⋆ Corporate Research (Control Engineering), Robert Bosch GmbH, 71272 Renningen, Germany (e-mail: {Steffen.Joos, Matthias.Bitzer2, Roland.Karrelmeyer}@de.bosch.com).
†Institute of Measurement, Control and Microtechnology, Ulm University, 89081 Ulm, Germany e-mail: knut.graichen@uni-ulm.de

978-3-9524-2699-9 ©2018 EUCA

are assumed, where $\boldsymbol{F}_x \in \mathbb{R}^{n_c \times n}$ and $\boldsymbol{g}_x(t) \in \mathbb{R}^{n_c}$ with

$$\boldsymbol{F}_x = \begin{bmatrix} \boldsymbol{f}_{x,1}, & \dots, & \boldsymbol{f}_{x,n_c} \end{bmatrix}^{\mathrm{T}}, \tag{2b}$$

$$\boldsymbol{g}_x(t) = \begin{bmatrix} g_{x,1}(t), & \dots, & g_{x,n_c}(t) \end{bmatrix}^{\mathrm{T}}. \tag{2c}$$

One can get an element-wise representation of the n_c state constraints according to

$$c_{x,k}(\boldsymbol{x}) := \boldsymbol{f}_{x,k}^{\mathrm{T}} \cdot \boldsymbol{x} - g_{x,k}(t) \leq 0, \; k = 1, \dots, n_c. \tag{2d}$$

Without loss of generality, the condition $g_{x,k}(t) \geq 0 \; \forall k$ is introduced. A state $\boldsymbol{x}$ satisfying (2) is called feasible. In addition to state constraints, a dynamic limitation

$$u_{\min}(t) \leq u(t) \leq u_{\max}(t) \tag{3}$$

of the control input $u(t)$ is taken into account. Moreover, the notation $b(i)$ is introduced which denotes in the following the i-th element of an arbitrary vector $\boldsymbol{b}$.

B. Flatness-based representation of constrained systems

Linear controllable systems (1) feature a flat output $z(t)$[1], since controllability and flatness are equivalent for linear systems [8]. With the property of flatness, the states $\boldsymbol{x}(t)$, the input $u(t)$, and the output $y(t)$ can be expressed as a function of the flat output $z(t)$ and its n time derivatives. Introducing the flat coordinates

$$\boldsymbol{z} = \begin{bmatrix} z, & \dot{z}, & \dots, & \overset{(n-1)}{z} \end{bmatrix}^{\mathrm{T}} = \begin{bmatrix} z_1, & z_2, & \dots, & z_n \end{bmatrix}^{\mathrm{T}}, \tag{4}$$

one obtains [7]

$$\boldsymbol{x}(t) = \boldsymbol{T}^{-1} \cdot \boldsymbol{z}(t), \tag{5}$$

$$u(t) = \left(\dot{z}_n(t) - \boldsymbol{t}^{\mathrm{T}} \cdot \boldsymbol{A}^n \cdot \boldsymbol{T}^{-1} \cdot \boldsymbol{z}(t)\right)/\beta, \tag{6}$$

$$y(t) = \boldsymbol{c}^{\mathrm{T}} \cdot \boldsymbol{T}^{-1} \cdot \boldsymbol{z}(t) \tag{7}$$

with $\beta = \boldsymbol{t}^{\mathrm{T}} \cdot \boldsymbol{A}^{(n-1)} \cdot \boldsymbol{b} \overset{!}{=} 1$ and the transformation matrix $\boldsymbol{T} = \begin{bmatrix} \boldsymbol{t}, & \boldsymbol{A}^{\mathrm{T}} \cdot \boldsymbol{t}, & \dots, & (\boldsymbol{A}^{\mathrm{T}})^{n-1} \cdot \boldsymbol{t} \end{bmatrix}^{\mathrm{T}}$.

The dynamic state constraints (2) can be expressed in flat coordinates using (5), i.e.

$$c_{z,k}(\boldsymbol{z}) := \boldsymbol{f}_{z,k}^{\mathrm{T}} \cdot \boldsymbol{z}(t) - g_{z,k}(t) \leq 0, \; k = 1, \dots, n_c \tag{8}$$

with $\boldsymbol{f}_{z,k}^{\mathrm{T}} = \boldsymbol{f}_{x,k}^{\mathrm{T}} \cdot \boldsymbol{T}^{-1}$ and $g_{z,k}(t) = g_{x,k}(t)$.

With respect to the control design discussed in the following, it is worth noting that the term $\boldsymbol{a}_{\mathrm{R}}^{\mathrm{T}} = \boldsymbol{t}^{\mathrm{T}} \cdot \boldsymbol{A}^n \cdot \boldsymbol{T}^{-1}$ in (6) corresponds to the last line of the system matrix $\boldsymbol{A}_{\mathrm{R}}$ [7] of the controllable canonical form

$$\dot{\boldsymbol{z}}(t) = \boldsymbol{A}_{\mathrm{R}} \cdot \boldsymbol{z}(t) + \boldsymbol{b}_{\mathrm{R}} \cdot u(t) \tag{9a}$$

$$y(t) = \boldsymbol{c}_{\mathrm{R}}^{\mathrm{T}} \cdot \boldsymbol{z}(t) \tag{9b}$$

of system (1), which can be computed with (5) and $\boldsymbol{A}_{\mathrm{R}} = \boldsymbol{T} \cdot \boldsymbol{A} \cdot \boldsymbol{T}^{-1}$, $\boldsymbol{b}_{\mathrm{R}} = \boldsymbol{T} \cdot \boldsymbol{b}$, and $\boldsymbol{c}_{\mathrm{R}}^{\mathrm{T}} = \boldsymbol{c}^{\mathrm{T}} \cdot \boldsymbol{T}^{-1}$.

III. Control design

For the purpose of stabilization and improved robustness against disturbances, a controller needs to be designed for the linear system (1). Thereby, the main difficulty lies in the satisfaction of the assumed constraints (2)-(3) for the states and the input. First, the design of state feedback controllers for unconstrained linear SISO systems is briefly revised in Sec. III-A. Then in Sec. III-B, the state feedback control concept is structurally extended such that an SFC is obtained. Therefore, Sec. III-C deals with the derivation of feasible dynamics in the constrained case while Sec. III-D discusses the stability of the derived (closed loop) dynamics and its dependency on the polytope geometry.

A. Unconstrained feedback control

In the following, the subject of (unconstrained) state feedback control is shortly discussed in terms of design and behavior. A well-known way to control linear SISO systems (1) is to apply state feedback

$$u_c = \boldsymbol{r}^{\mathrm{T}} \cdot (\boldsymbol{x}^* - \boldsymbol{x}) = \boldsymbol{r}^{\mathrm{T}} \cdot \boldsymbol{e}. \tag{10}$$

Thereby, the control error $\boldsymbol{e}(t)$, i.e. the deviation between a desired state vector $\boldsymbol{x}^*(t)$ available from e.g. a trajectory planning [6] and the state $\boldsymbol{x}$, which is required to be known using measurements or a state observer, is asymptotically stabilized. For the now considered unconstrained case, the controller parameters $\boldsymbol{r}$ can be calculated using well-known control concepts as e.g. pole placement or a linear quadratic regulator (LQR), see e.g. [12], such that the closed loop system $\dot{\boldsymbol{x}} = (\boldsymbol{A} - \boldsymbol{b} \cdot \boldsymbol{r}^{\mathrm{T}}) \cdot \boldsymbol{x} + \boldsymbol{b} \cdot \boldsymbol{r}^{\mathrm{T}} \cdot \boldsymbol{x}^*$ is asymptotically stable. This is the case when the eigenvalues of the closed loop system matrix $(\boldsymbol{A} - \boldsymbol{b} \cdot \boldsymbol{r}^{\mathrm{T}})$ have a negative real part.

The consideration of the constraints (2) and (3) requires additional care in the design of the controller (10). A naive approach to deal with the constraints is to choose the controller parametrization conservatively such that a slow controller performance results. However, this is not acceptable for most control tasks. Hence, a method for dealing with the constraints in a more optimal manner is derived in the sequel such that both constraint satisfaction and a sufficiently aggressive control performance is achieved.

B. Structure of constrained SFC

The goal of the presented approach is to use the state feedback controller (10), which is tuned for high performance, as long as the constraints (2) and (3) are satisfied. In the case when (10) leads to an infeasible control signal u_c due to actuator saturation or a violation of state constraints, a feasible control, i.e. a limited input signal $u_{c,\mathrm{Lim}}$, has to be derived. In order to both judge if u_c is feasible and to calculate $u_{c,\mathrm{Lim}}$, the property of differential flatness is exploited as a transformation between the state space models (1) and (9). More precisely, the inverse flatness-based input parametrization (IIP) $\dot{z}_n(t) = \boldsymbol{a}_{\mathrm{R}}^{\mathrm{T}} \cdot \boldsymbol{z}(t) + u(t)$, which corresponds to the last line of (9a), is utilized to determine the desired highest derivative $\dot{z}_n = \gamma_{c,\mathrm{D}}(\boldsymbol{z}, u_c)$ adjusted by the controller (10) for the unconstrained case according to

$$\dot{z}_n(t) = \gamma_{c,\mathrm{D}}(\boldsymbol{z}, u_c) := \boldsymbol{a}_{\mathrm{R}}^{\mathrm{T}} \cdot \boldsymbol{z}(t) + u_c(t). \tag{11}$$

This means that for the adjustment of $\gamma_{c,\mathrm{D}} \to \gamma_{c,\mathrm{Lim}}$, see Fig. 2, the original system (1) is reduced to an integrator chain (4) of order n as depicted in Fig. 3. The resulting problem is then to control the integrator chain (4) such that the constraints (8) and (3) are satisfied which leads to the limited highest derivative $\dot{z}_n = \gamma_{c,\mathrm{Lim}}$, see Fig. 2. The actual limitation by means of an optimization problem leads to an SFC and is discussed in Sec. IV. The input parametrization (IP) (6)

$$u_{c,\mathrm{Lim}}(t) = \gamma_{c,\mathrm{Lim}}(t) - \boldsymbol{a}_{\mathrm{R}}^{\mathrm{T}} \cdot \boldsymbol{z}(t) \tag{12}$$

[1] One can explicitly calculate the flat output $z(t) = \boldsymbol{t}^{\mathrm{T}} \cdot \boldsymbol{x}(t)$ choosing $\boldsymbol{t}^{\mathrm{T}} = \begin{bmatrix} 0, & 0, & \dots, & 0, & \beta \end{bmatrix} \cdot \boldsymbol{Q}_{\mathrm{S}}^{-1}$ according to the last line of the inverse controllability matrix $\boldsymbol{Q}_{\mathrm{S}}$ [7].

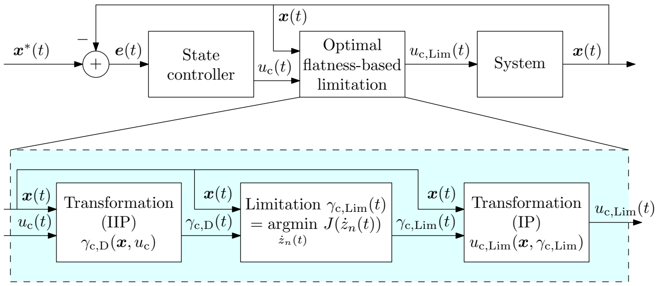

Fig. 2. Principle structure of the (optimal) flatness-based limitation of the control signal u_c with the transformations (11)-(12).

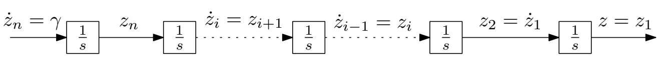

Fig. 3. Integrator chain (4) with n states.

then allows the conversion of the (optimally) modified $\gamma_{c,\mathrm{Lim}}$ to a limited input signal $u_{c,\mathrm{Lim}}$ in accordance to Fig. 2. The resulting control task has similarities with the constrained trajectory planning problem [6]. Hence, the idea from [6] is used in the sequel as a basis in order to derive an optimization-based constrained feedback control approach.

C. Derivation of feasible limits for the integrator chain input

As discussed in the previous section, the property of flatness (5)-(6) is utilized in conjunction with (3) and (8) for the calculation of dynamic limits of the integrator chain's input $\dot{z}_n = \gamma$. More precisely, in order to achieve a feasible closed loop system behavior, lower and upper limits $\gamma_\ominus \leq \gamma \leq \gamma_\oplus$ are required, whereas $\gamma_\ominus$, $\gamma_\oplus$ are designed as a dedicated control law by means of each of the constraints. In order to systematically derive suitable control laws resp. limits, the present section deals with the reformulation of the constraints (3) and (8) in dependance of the highest derivative $\dot{z}_n(t)$, see also [6], such that the following equation structure is obtained:

$$-\dot{z}_n + \gamma_\ominus(\boldsymbol{z}) \leq 0, \quad \dot{z}_n - \gamma_\oplus(\boldsymbol{z}) \leq 0. \tag{13}$$

In a first step, it is known from [6] and [13] that the input constraints (3) can be formulated with (6) according to

$$-\dot{z}_n(t) + \gamma_{\ominus,\mathrm{in}}(\boldsymbol{z}, u_{\min}) \leq 0, \tag{14a}$$
$$\dot{z}_n(t) - \gamma_{\oplus,\mathrm{in}}(\boldsymbol{z}, u_{\max}) \leq 0 \tag{14b}$$

as a function of $\dot{z}_n(t)$ with the dynamic limits

$$\gamma_{\ominus,\mathrm{in}}(\boldsymbol{z}, u_{\min}) = \boldsymbol{a}_\mathrm{R}^\mathrm{T} \cdot \boldsymbol{z}(t) + u_{\min}(t), \tag{15a}$$
$$\gamma_{\oplus,\mathrm{in}}(\boldsymbol{z}, u_{\max}) = \boldsymbol{a}_\mathrm{R}^\mathrm{T} \cdot \boldsymbol{z}(t) + u_{\max}(t). \tag{15b}$$

Note that the resulting limits (15) ensuring the input constraints (3) represent the last row of the system dynamics (9a) stimulated with the input limits $u_{\min}(t)$ or $u_{\max}(t)$.

As a second step, feasible dynamics for the flatness-based state constraints (8) are derived. The idea is to calculate a limited dynamics in such a manner that the states $\boldsymbol{z}$ are steered on resp. along the state constraints, i.e. along the boundary of a polytope, see the sketch in Fig. 4.

A generalized approach for deriving feasible γ_k with respect to the (time-variant) constraints (8) is presented in the following such that a stable system behavior is obtained when the respective γ_k is active. This can be achieved by

$$\gamma_k(t) = w_k(t) - \boldsymbol{r}_k^\mathrm{T} \cdot \boldsymbol{z} \tag{16}$$

which has the form of a control law and which stabilizes the state $\boldsymbol{z}$ on the respective k-th state constraint. Thereby, it is irrelevant if the state $\boldsymbol{z}$ is still within the feasible area or has already left the feasible area due to an overshoot. In order to derive the unknown controller parameters $\boldsymbol{r}_k$ and $w_k(t)$, the definition of the index ξ_k of the k-th constraint (8) is introduced as

$$\xi_k = \min_i \quad r_i \qquad \text{s.t.} \quad r_i = n + 1 - i, \quad f_{z,k}(i) \neq 0, \quad 1 \leq i \leq n, \tag{17}$$

where ξ_k represents the index i of the state z_i that has both minimum relative degree and influences the k-th constraint (8) which then reads as (since $f_{z,k}(i) = 0, \forall\ \xi_k < i \leq n$)

$$f_{z,k}(1) \cdot z_1(t) + \cdots + f_{z,k}(\xi_k) \cdot z_{\xi_k}(t) - g_{z,k}(t) \leq 0. \tag{18}$$

With the knowledge of the index ξ_k, the feedback gain $\boldsymbol{r}_k$ (16) that stabilizes all states z_i with $\xi_k \leq i \leq n$ can be designed, e.g. with pole placement. Thereby, $n - \xi_k + 1$ eigenvalues with negative real part are set while the remaining $\xi_k - 1$ poles are left untouched at 0, resulting in the characteristic polynomial

$$\lambda^{(\xi_k - 1)} \cdot \left(a_{(n-\xi_k+1)} \cdot \lambda^{(n-\xi_k+1)} + \cdots + a_1 \cdot \lambda + a_0 \right) \tag{19}$$

and leading to the feedback gain structure

$$\boldsymbol{r}_k = \begin{bmatrix} 0, & \ldots, & 0, & r_k(\xi_k), & \ldots, & r_k(n) \end{bmatrix}^\mathrm{T}. \tag{20}$$

The reference $w_k(t)$ in (16) needs to be formulated for the state z_{ξ_k} such that the state is driven on resp. along the k-th constraint, recall Fig. 4. Therefore, the k-th constraint (18) is solved for z_{ξ_k} in the limiting case and rewritten as

$$w_k(t) \stackrel{!}{=} r_k(\xi_k) \cdot z_{\xi_k}(t) := w_{\mathrm{p},k}(t) - \boldsymbol{r}_{\mathrm{p},k}^\mathrm{T} \cdot \boldsymbol{z} \tag{21}$$

with

$$w_{\mathrm{p},k}(t) = \frac{r_k(\xi_k)}{f_{z,k}(\xi_k)} \cdot g_{z,k}(t), \tag{22}$$

$$\boldsymbol{r}_{\mathrm{p},k} = r_k(\xi_k) \cdot \begin{bmatrix} \frac{f_{z,k}(1)}{f_{z,k}(\xi_k)}, \ldots, \frac{f_{z,k}(\xi_k - 1)}{f_{z,k}(\xi_k)}, 0, \ldots, 0 \end{bmatrix}^\mathrm{T}. \tag{23}$$

Note, that $\boldsymbol{r}_{\mathrm{p},k}$ is generally time-invariant and in the case of a box constraint it is given as $\boldsymbol{r}_{\mathrm{p},k} = \mathbf{0}$. Furthermore, the scalar $f_{z,k}(\xi_k)$ (18) allows a classification of the k-th constraint according to its sign, i.e. $\mathrm{sign}(f_{z,k}(\xi_k)) \in \{-1, 1\}$, such that two different types of inequalities (13)

$$-\dot{z}_n(t) + \gamma_{\ominus,k_-}(\boldsymbol{z}, w_{\mathrm{p},k_-}) \leq 0, \quad k_- = 1, \ldots, n_{c,-}, \tag{24a}$$
$$\dot{z}_n(t) - \gamma_{\oplus,k_+}(\boldsymbol{z}, w_{\mathrm{p},k_+}) \leq 0, \quad k_+ = 1, \ldots, n_{c,+} \tag{24b}$$

with $n_{c,-} + n_{c,+} = n_c$ are obtained from (16). Thereby, the state vector dependent lower and upper limits (24)

$$\gamma_{\ominus,k_-}(\boldsymbol{z}, w_{\mathrm{p},k_-}) = w_{\mathrm{p},k_-}(t) - (\boldsymbol{r}_{k_-}^\mathrm{T} + \boldsymbol{r}_{\mathrm{p},k_-}^\mathrm{T}) \cdot \boldsymbol{z}, \tag{25a}$$
$$\gamma_{\oplus,k_+}(\boldsymbol{z}, w_{\mathrm{p},k_+}) = w_{\mathrm{p},k_+}(t) - (\boldsymbol{r}_{k_+}^\mathrm{T} + \boldsymbol{r}_{\mathrm{p},k_+}^\mathrm{T}) \cdot \boldsymbol{z} \tag{25b}$$

are composed of (20), (22)-(23), and depend only on the polytope (2) and the parameters of the designed stabilizing controller $\boldsymbol{r}_k$ (20).

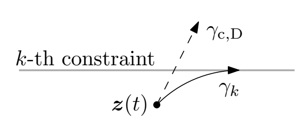

Fig. 4. Sketch of the state $\boldsymbol{z}(t)$ approaching the state constraint k. The application of $\dot{z}_n = \gamma_{c,D}$ (dashed line) and $\dot{z}_n = \gamma_k$ (solid line) lead to infeasible and feasible trajectories respectively.

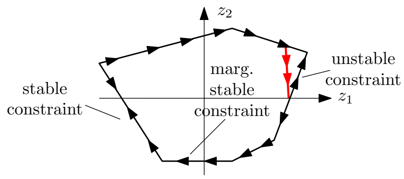

Fig. 5. Qualitative illustration of the manipulation (red) of the polytope (8) in order to obtain a feasible series of constraints. The arrows represent the feasible directions according to the vector field given by the integrator chain.

D. Remarks on polytope geometry, constrained dynamics, and its stability

Recalling the idea of Sec. III-A – III-C of modifying the feedback (10) in such a way that the state trajectory (ST) is driven along the constraint, it is of interest whether the dynamic behavior in the limiting case is stable and how the course of the ST changes with the intersection of subsequent state constraints. Therefore, the current section qualitatively discusses these two aspects and points out a link of the closed loop system stability with the geometry of the polytope (2a).

In the case of an active state constraint (8), the closed loop system is given by the integrator chain (4) controlled with (25) according to

$$\dot{\boldsymbol{z}} = \begin{bmatrix} \boldsymbol{0}, & \boldsymbol{I} \\ -(\boldsymbol{r}_k^{\mathrm{T}} + \boldsymbol{r}_{\mathrm{p},k}^{\mathrm{T}}) & \end{bmatrix} \cdot \boldsymbol{z} + \begin{bmatrix} \boldsymbol{0} \\ 1 \end{bmatrix} \cdot w_{\mathrm{p},k}(t). \qquad (26)$$

Since $\boldsymbol{r}_k$ (20) is calculated such that the states z_i with $\xi_k \leq i \leq n$ are stabilized by design, the stability only depends on $\boldsymbol{r}_{\mathrm{p},k}$ (23). This means that the stability of (26) is influenced only by the geometry of the k-th polytopic constraint (8).

A possibility to exemplify this fact is to consider the polytopic constraint as a manifold in the n-dimensional flat state space $\mathbb{R}^n$. The direction on which the ST can be steered along that manifold is uniquely defined by the vector field of the integrator chain (4) in each sector of the space $\mathbb{R}^n$. Consequently, in terms of the equilibrium line, i.e. the z_1-axis, there exist three different possibilities for the running direction of the ST on the k-th constraint. The respective direction in turn influences both the resulting $\boldsymbol{r}_{\mathrm{p},k}$ (23) and finally the stability of (26) leading to the following conventions:

1) The ST converges to the z_1-axis: Then, $\boldsymbol{r}_{\mathrm{p},k}$ leads to a stable system (26), i.e. 'k is a stable constraint'.
2) The ST runs parallel to the z_1-axis: Then, $\boldsymbol{r}_{\mathrm{p},k}$ leads to a marginally stable system (26), i.e. 'k is a marginally stable constraint' (as in the case of box constraints).
3) The ST diverges from the z_1-axis: Then, $\boldsymbol{r}_{\mathrm{p},k}$ leads to an unstable system (26), i.e. 'k is an unstable constraint'.

Fig. 5 gives an exemplary graphic illustration in two dimensions. With the above introduced stability classification of the constraints, respective rules for the geometry of the polytope in flat coordinates (8) can be specified that have to be obeyed in order to avoid a globally diverging behavior of the switched system, i.e. an unstable running direction of the ST. These rules postulate that

- a (series of) unstable constraint(s) has to intersect with at least one (marginally) stable constraint. And,
- a (series of) marginally stable constraint(s) has to intersect with at least one stable constraint.

If these two necessary conditions are not fulfilled, as it is the case in the example shown in Fig. 5, the polytope has to be manipulated such that the introduced conditions hold. This can e.g. be achieved by cutting off the problematic sectors, which is equivalent to the introduction of additional stable constraints, as sketched in Fig. 5 with the red line.

IV. Derivation of (optimal) switched feedback controller (SFC)

The constrained control problem in consideration is expressed as an optimization problem for the derivation of the SFC in Sec. IV-A and discussed with respect to its solvability and feasibility. In Sec. IV-B, a solution of the optimization problem is specified and extended for a prioritization of constraints in order to transparently handle potentially occurring (temporarily) infeasible situations.

A. Set-up of optimization problem

For the derivation of an optimal SFC, the above objectives for high performance and constraint satisfaction are formulated as an optimization problem. A possible objective function results from the optimal tracking of the unconstrained control signal (10), i.e. $u(t) \to u_{\mathrm{c}}(t)$, in order to assure high performance. The optimization variable is obviously the highest order derivative $\dot{z}_n(t) = \gamma$ representing the input of the integrator chain (4). Therefore, the objective function is chosen as the quadratic deviation of $\gamma_{\mathrm{c,D}}(\boldsymbol{z}, u_{\mathrm{c}})$ (11) for the unconstrained case and the optimization variable $\dot{z}_n$. The optimization constraints have the form (13) and are set up according to (14) and (24).

This results in a scalar optimization problem:

$$\begin{aligned} \gamma_{\mathrm{c,Lim}}(t) = \ & \underset{\dot{z}_n}{\operatorname{argmin}} \ \left(\gamma_{\mathrm{c,D}}(\boldsymbol{z}, u_{\mathrm{c}}) - \dot{z}_n \right)^2 && (27) \\ \text{w.r.t.} \quad & -\dot{z}_n + \gamma_{\ominus,k_-}(\boldsymbol{z}, w_{\mathrm{p},k_-}) \leq 0, \forall k_- \\ & -\dot{z}_n + \gamma_{\ominus,\mathrm{in}}(\boldsymbol{z}, u_{\min}) \leq 0 \\ & \dot{z}_n - \gamma_{\oplus,k_+}(\boldsymbol{z}, w_{\mathrm{p},k_+}) \leq 0, \forall k_+ \\ & \dot{z}_n - \gamma_{\oplus,\mathrm{in}}(\boldsymbol{z}, u_{\max}) \leq 0. \end{aligned}$$

The feasibility and solvability of (27) can not be guaranteed $\forall \boldsymbol{z}(t)$. Depending on the situation, the time-variant constraints of (27) might become temporarily contradictory. This is e.g. the case if $\exists\, k_-$ and some time interval $t \in (t_1, t_2)$ such that $\gamma_{\oplus,\mathrm{in}}(\boldsymbol{z}, u_{\max}) < \gamma_{\ominus,k_-}(\boldsymbol{z}, w_{\mathrm{p},k_-})$. Consequently, this case exemplifies that the necessary actuator energy is not available and the dynamics required for the satisfaction of a respective state constraint k_- can not be realized due to the actuator saturation.[1] Therefore, in order to achieve an implementable solution which both leads to a fast feedback behavior, i.e. for aggressive tuning of $\boldsymbol{r}$ (10), and is viable $\forall t$, a prioritization of the constraints within the optimization problem (27) is necessary which is introduced next.

B. Incorporation of constraints prioritization

Infeasible situations with contradicting constraints as previously described require a decision which constraint is ensured resp. violated. In order to handle such situations transparently, an order of constraints prioritization is necessary. Hence, for the considered state and input constraints, the constraints on the input have the highest priority whereas constraints on the states have decreasing priority towards

[1] It is possible to theoretically obtain a feasible problem (27) $\forall t$. This can especially be achieved for a very conservative tuning of the state controller (10) leading to a quasi-static system behavior as described in [14].

the integrator chain output. In the following, the introduced prioritization of the constraints is incorporated in the optimal solution of problem (27).

It is known, see e.g. [6], [13], that the solution of a scalar optimization problem (27) has the structure of a limiting characteristic element (LE) which reads for the specific problem (27) as

$$\gamma_{\mathrm{c,Lim}}(t) = \begin{cases} \gamma_{\ominus}(t), & \gamma_{\mathrm{c,D}} < \gamma_{\ominus} \\ \gamma_{\mathrm{c,D}}(\boldsymbol{z}, u_{\mathrm{c}}), & \gamma_{\ominus} \leq \gamma_{\mathrm{c,D}} \leq \gamma_{\oplus} \\ \gamma_{\oplus}(t), & \gamma_{\mathrm{c,D}} > \gamma_{\oplus}, \end{cases} \tag{28}$$

with $\gamma_{\mathrm{c,D}}(\boldsymbol{z}, u_{\mathrm{c}})$ given by the unconstrained controller (11) and the dynamic limits

$$\gamma_{\ominus}(t) \in \left\{\gamma_{\ominus,\mathrm{in}}, \gamma_{\ominus,1}, \ldots, \gamma_{\ominus,n_{\mathrm{c},-}}\right\}, \tag{29a}$$

$$\gamma_{\oplus}(t) \in \left\{\gamma_{\oplus,\mathrm{in}}, \gamma_{\oplus,1}, \ldots, \gamma_{\oplus,n_{\mathrm{c},+}}\right\} \tag{29b}$$

in accordance to the limits γ derived in Sec. III-C. In order to avoid $\gamma_{\ominus} > \gamma_{\oplus}$ in (28)-(29), the above introduced prioritization of the constraints is incorporated in the solution (28). Therefore, a straight-forward approach is to substitute the (single) LE (28) with a cascade of $n_{\mathrm{Lim}}+1$ LEs as sketched in Fig. 6. Thereby, one LE for the input constraints as well as an additional LE per integrator state z_i, $i = 1, \ldots, n$ for which $\exists\, \xi_k = i$ is implemented, see (17). While the limits for the last (highest prioritized) LE are uniquely given by the dynamic limits (15) for the input, the limits of the remaining $n_{\mathrm{Lim}} \leq n_{\mathrm{c}}$ LEs representing the state constraints have to be chosen from a respective set of relevant candidates (24). 'Relevant' means in terms of the $j = 1, \ldots, n_{\mathrm{Lim}}$-th LE that the corresponding index of the k-th constraint $\xi_k = j$ is equal to j. The dynamic limits relevant for the j-th LE are denoted with $\gamma_{\ominus,k_-|\xi_{k_-}=j}$ and $\gamma_{\oplus,k_+|\xi_{k_+}=j}$, respectively. The selection of the optimal dynamic limit out of each set of candidates $\gamma_{\ominus,k_-|\xi_{k_-}=j}$ and $\gamma_{\oplus,k_+|\xi_{k_+}=j}$ can then be simplified to a max- and min-search problem

$$\gamma_{\ominus,\mathrm{act}|\xi=j} = \max\left\{\gamma_{\ominus,k_-|\xi_{k_-}=j}\right\}, \tag{30a}$$

$$\gamma_{\oplus,\mathrm{act}|\xi=j} = \min\left\{\gamma_{\oplus,k_+|\xi_{k_+}=j}\right\} \tag{30b}$$

which is solved for each time instant t. Furthermore, it is assumed that all LEs in Fig. 6 are well defined which means that the respective lower limit is smaller than the upper limit.

V. Examples

For the demonstration of the performance of the derived SFC approach, two different set-ups of the control scheme are considered in a simulation study. In the first scenario pure state feedback is applied using the SFC in order to show feasibility, robustness and optimal behavior of the SFC for a stabilization example around the origin. Then in the second scenario, the SFC is used within a constrained 2DOF-structure. Thereby, the subject of the SFC is the stabilization of a feedforwarded constrained reference trajectory generated online with the switched state variable filter concept [6] which requires the SFC to deal with time-varying constraints. For both simulation scenarios, the SFC is benchmarked with an (optimal) MPC feedback controller calculated with the toolbox ACADO [15].

In the following, the plant under consideration is an unstable first-order lag element followed by an integrator given in the controllable canonical form

$$\dot{\boldsymbol{x}}(t) = \begin{bmatrix} 0 & 1 \\ 0 & 1 \end{bmatrix} \cdot \boldsymbol{x}(t) + \begin{bmatrix} 0 \\ 1 \end{bmatrix} \cdot u(t) + \boldsymbol{e}(t) \tag{31a}$$

$$y(t) = \begin{bmatrix} 1, & 0 \end{bmatrix} \cdot \boldsymbol{x}(t). \tag{31b}$$

The unknown disturbance $\boldsymbol{e}(t)$ (31a) is chosen according to

$$\boldsymbol{e}(t) = \begin{cases} \begin{bmatrix} 0.2, & 0.3 \end{bmatrix}^{\mathrm{T}}, & t < 6\,\mathrm{s} \\ \begin{bmatrix} 0\;, & 0 \end{bmatrix}^{\mathrm{T}}, & 6\,\mathrm{s} \leq t \leq 9\,\mathrm{s},\ t \geq 13\,\mathrm{s} \\ \begin{bmatrix} -0.2, & 0.3 \end{bmatrix}^{\mathrm{T}}, & 9\,\mathrm{s} < t < 13\,\mathrm{s} \end{cases} \tag{32}$$

while the assumed initial value $\boldsymbol{x}(0) = \boldsymbol{x}_0$ is inaccurate with

$$\boldsymbol{x}(0) = \boldsymbol{x}_0 + \Delta\boldsymbol{x}_0 = \begin{bmatrix} 0, & 0 \end{bmatrix}^{\mathrm{T}} + \begin{bmatrix} -0.9, & -0.15 \end{bmatrix}^{\mathrm{T}}. \tag{33}$$

Furthermore, the input constraints

$$-1 \leq u(t) \leq 1 \tag{34}$$

as well as polytopic state constraints P_x (2a) according to

$$\boldsymbol{F}_x = \begin{bmatrix} 1, & 0, & -1, & 0, & -0.316, & 0.371, & -0.196, & 0.196 \\ 0, & 1, & 0, & -1, & 0.949, & 0.929, & -0.981, & -0.981 \end{bmatrix}^{\mathrm{T}},$$

$$\boldsymbol{g}_x = \begin{bmatrix} 1.5, & 0.4, & 1, & 0.4, & 0.506, & 0.631, & 0.353, & 0.549 \end{bmatrix}^{\mathrm{T}}, \tag{35}$$

are taken into account. For the asymptotic stabilization of the disturbed system towards the origin $\boldsymbol{x}^* = \boldsymbol{0}$, the eigenvalues $\lambda_1 = 0$, $\lambda_2 = 1$ of the undisturbed system (31) are moved to $\lambda_{1/2} = -4$ using the state feedback controller (10) which can e.g. be designed by means of the well-known Ackermann formula [12]. The respective stabilizing controllers for the state constraints (35) are tuned very fast with eigenvalues specified at $\lambda = -600$.

The results for the first scenario with pure state feedback are illustrated in Fig. 7 for the described constraint and disturbance scenario (32)-(35). Thereby, neither the input constraints nor the state constraints are violated and the system is stabilized which can be seen in the left phase portrait in Fig. 9. It can be asserted especially in the plot of the input $u(t)$ that the blue lines representing the SFC approximates the red-dashed MPC[1] behavior, which is considered as benchmark. However note that in order to achieve stationary exactness during the presence of disturbances an integral part would be required for both the SFC and MPC. For the simulation of the constrained 2DOF-structure in the

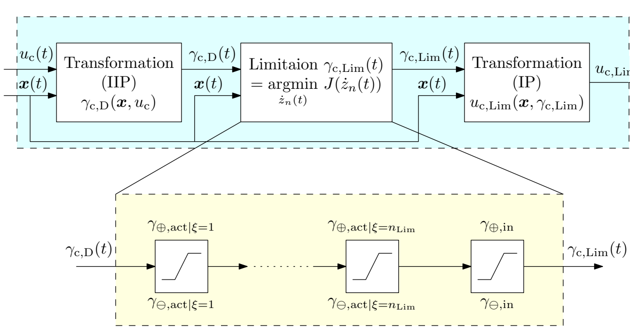

Fig. 6. Structure of the optimal, prioritization-based limitation of the signal $\gamma_{\mathrm{c,D}}$ calculated by the feedback controller (10).

[1] All red curves below are generated online with ACADO [15] using a prediction horizon of 0.01 s corresponding to 10 samples of the fixed simulation step size of 0.001 s and the cost function $J = \frac{1}{2} \cdot \int 5 \cdot (x_1(t) - x_1^*(t))^2 + 0.01 \cdot (x_2(t) - x_2^*(t))^2\, \mathrm{d}t$.

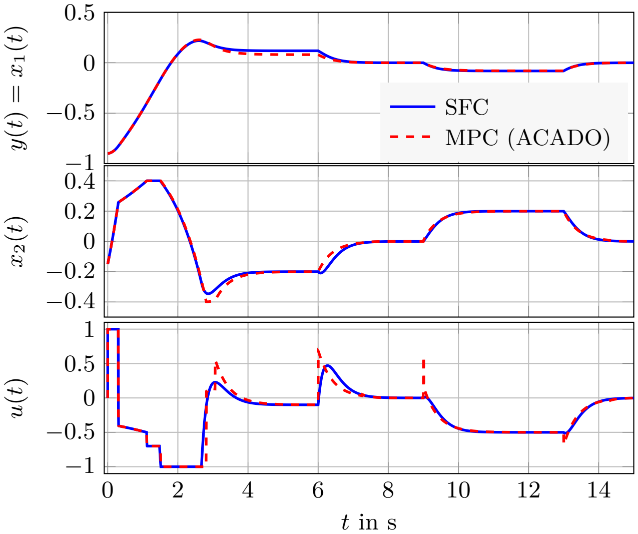

Fig. 7. Simulation results for the first scenario with pure state feedback. The constraints are set according to (34) and (35).

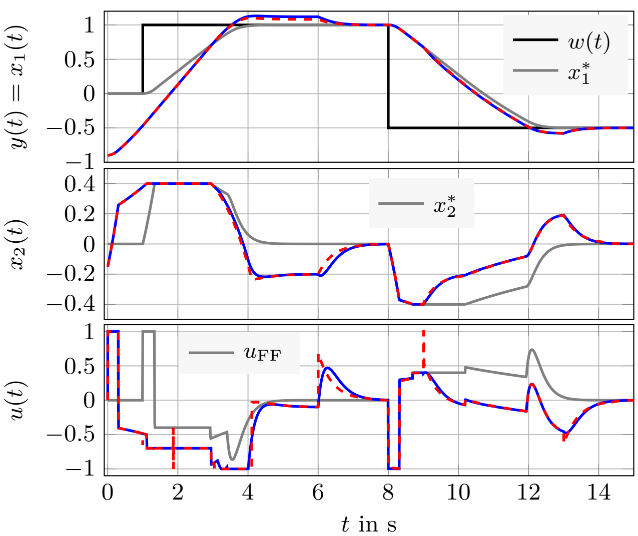

Fig. 8. Simulation results for the second scenario using a constrained 2DOF-setup to solve a constrained set-point tracking task.

second scenario, the system, the disturbances, and the system constraints remain unchanged, i.e. as already introduced. However, the desired state trajectories x_1^*, x_2^* as well as the feedforward signal u_{FF} are now calculated by means of the approach discussed in [6]. These desired signals (gray lines) together with the states $\boldsymbol{x}$ of the closed loop system are depicted in Fig. 8 and the right phase portrait of Fig. 9. Note that the manipulated input signal is given by $u = u_{\mathrm{c,Lim}} + u_{\mathrm{FF}}$ due to the 2DOF-structure. Both figures show a robust and feasible tracking of the set points according to the black reference $w(t)$ (or the green dots in Fig. 9 right), i.e. without violation of any constraints. Furthermore, it is worth noting that in order to achieve the illustrated performance both feedback control approaches (SFC and MPC) have to deal with time-varying input and state constraints, since the dynamic quantities x_1^*, x_2^* and u_{FF} have to be taken into account for the calculation of a feasible feedback control signal.

VI. Conclusion

In this contribution, a novel constructive switched feedback control (SFC) approach for dealing with both input

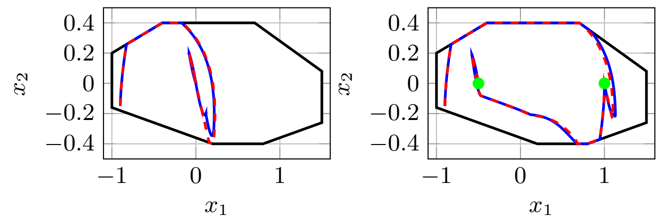

Fig. 9. Phase portrait and polytope for the scenarios of Fig. 7-8.

and state constraints is derived for linear system dynamics. Simulation studies show that if tuned sufficiently fast, a control performance almost identical to MPC can be achieved with the presented approach. Due to the prioritization-based concept, the implementation is straightforward and iteration-free and is therefore especially promising for highly dynamic applications. However, this comes with the trade-off of an overshoot, i.e. a possible violation of constraints in the case of too aggressive tuning or when control energy is not sufficiently available. Furthermore, the control concept is designed in such a way that it accepts time-varying constraints which means that the SFC concept is suitable for the synthesis of a constrained two-degree-of-freedom structure together with a (constrained) feedforward control approach. Interesting aspects for future work include the extension of the control concept for the nonlinear flat case, the investigation of the SFC approach for practical problems, as well as approaches for stability considerations of the closed-loop switched system.

References

[1] J. Adamy and A. Flemming, "Soft variable-structure controls: a survey," *Automatica*, vol. 40, pp. 1821–1844, 2004.

[2] F. Borrelli, A. Bemporad, and M. Morari, "Predictive control for linear and hybrid systems," *Cambridge University Press*, 2011.

[3] B. Käpernick and K. Graichen, "Nonlinear model predictive control based on constraint transformation," *Optimal Control Applications and Methods*, vol. 37, no. 4, pp. 807 – 828, 2016.

[4] O. J. Rojas and G. C. Goodwin, "A simple anti-windup strategy for state constrained linear control," in *Proceedings of the 15th IFAC World Congress*, 2002, pp. 109–114.

[5] P. Hippe, *Windup in Control*. Springer, 2006.

[6] S. Joos, M. Bitzer, R. Karrelmeyer, and K. Graichen, "Online-trajectory planning for state- and input-constrained linear SISO systems using a switched state variable filter," in *Proceedings 20th IFAC World Congress*, 2017, pp. 2639–2644.

[7] H. Sira-Ramirez and S. K. Agrawal, *Differentially Flat Systems*. CRC Press, 2004.

[8] M. Fliess, J. Lévine, P. Martin, and P. Rouchon, "Flatness and defect of non-linear systems: introductory theory and examples," *International Journal of Control*, vol. 61, pp. 1327–1361, 1995.

[9] J. Nocedal and S. J. Wright, *Numerical Optimization*. Springer, 2006, Second Edition.

[10] M. Johansson, *Piecewise Linear Control Systems*. Springer, 2003.

[11] A. Isidori, *Nonlinear Control Systems*. Springer, 1995.

[12] R. C. Dorf and R. H. Bishop, *Modern Control Systems*. Prentice Hall, 2011, 12th Edition.

[13] P. Kotman, M. Bitzer, and A. Kugi, "Prioritization-Based Constrained Trajectory Planning for a Nonlinear Turbocharged Air System with EGR," in *Proceedings of the American Control Conference*, 2012, pp. 5712–5717.

[14] T. Faulwasser, V. Hagenmeyer, and R. Findeisen, "Constrained reachability and trajectory generation for flat systems," *Automatica*, vol. 50, pp. 1151–1159, 2014.

[15] D. Ariens, M. Diehl, H. J. Ferreau, B. Houska, F. Logist, R. Quirynen, and M. Vukov, "ACADO Toolkit User's Manual," http://acado.sourceforge.net/doc/pdf/acado_manual.pdf, 2014.